HAL
open science

Evaluation of cobalt free coatings as hardfacing material candidates in sodium-cooled fast reactor and effect of oxygen in sodium on the tribological behaviour

Fabien Rouillard, Brigitte Duprey, Jean-Louis Courouau, Raphaël Robin, Pascal Aubry, Cécile Blanc, Michel Tabarant, Hicham Maskrot, Laetitia Nicolas, Martine Blat-Yrieix, et al.

To cite this version:

Fabien Rouillard, Brigitte Duprey, Jean-Louis Courouau, Raphaël Robin, Pascal Aubry, et al.. Evaluation of cobalt free coatings as hardfacing material candidates in sodium-cooled fast reactor and effect of oxygen in sodium on the tribological behaviour. EPJ N - Nuclear Sciences & Technologies, 2019, 5, pp.10. 10.1051/epjn/2019025 . cea-02458447

HAL Id: cea-02458447

https://cea.hal.science/cea-02458447v1

Submitted on 29 Jan 2020

HAL is a multi-disciplinary open access archive for the deposit and dissemination of scientific research documents, whether they are published or not. The documents may come from teaching and research institutions in France or abroad, or from public or private research centers.

L'archive ouverte pluridisciplinaire **HAL**, est destinée au dépôt et à la diffusion de documents scientifiques de niveau recherche, publiés ou non, émanant des établissements d'enseignement et de recherche français ou étrangers, des laboratoires publics ou privés.

EPJ Nuclear Sci. Technol. **5**, 10 (2019)
© F. Rouillard et al., published by EDP Sciences, 2019
https://doi.org/10.1051/epjn/2019025

EPJ Nuclear Sciences & Technologies

Available online at:
https://www.epj-n.org

Regular Article

Open Access

Evaluation of cobalt free coatings as hardfacing material candidates in sodium-cooled fast reactor and effect of oxygen in sodium on the tribological behaviour

Fabien Rouillard[1,*], Brigitte Duprey[1], Jean-Louis Courouau[1], Raphaël Robin[1], Pascal Aubry[2], Cécile Blanc[2], Michel Tabarant[2], Hicham Maskrot[2], Laetitia Nicolas[3], Martine Blat-Yrieix[4], Gilles Rolland[4], and Thorsten Marlaud[5]

[1] Den-Service de la Corrosion et du Comportement des Matériaux dans leur Environnement (SCCME), CEA, Université Paris-Saclay, 91191 Gif-sur-Yvette, France
[2] Den-Service d'Etudes Analytiques et de Réactivtiés des Surfaces (SEARS), CEA, Université Paris-Saclay, 91191 Gif-sur-Yvette, France
[3] Den-Service de Recherches Métallurgiques Appliquées (SRMA), CEA, Université Paris-Saclay, 91191 Gif-sur-Yvette, France
[4] EDF R&D, Département Matériaux et Mécanique des Composants, Les Renardières, 77818 Moret Loing Orvanne, France
[5] FRAMATOME, DTIML, 10 rue Juliette Récamier, 69006 Lyon, France

Received: 11 February 2019 / Received in final form: 20 May 2019 / Accepted: 2 August 2019

Abstract. The feedback produced by operating Sodium-cooled Fast Reactors (SFRs) has shown the importance of material tribological properties. Where galling or adhesive wear cannot be allowed, hardfacing alloys, known to be galling-resistant coatings, are usually applied on rubbing surfaces. The most used coating is the cobalt-base alloy named Stellite 6® because of its outstanding friction and wear behaviour. Nevertheless, cobalt is an element which activates in the reactor leading to complex management of safety during reactor maintenance and mainly decommissioning. As a consequence, a collaborative work between CEA, EDF and FRAMATOME has been launched for selecting promising cobalt-free hardfacing alloys for the 600 MWe Sodium-cooled Fast breeder reactor project named ASTRID. Several nickel-base alloys have been selected from literature review then deposited by Plasma Transferred Arc or Laser Cladding on 17Cr austenitic stainless steel 316L(N) according to RCC-MRx Code (AFCEN Code). Among the numerous properties required for qualifying their use as hardfacing alloys in SFR, good corrosion behaviour and good friction and wear behaviour in sodium are essential. First results on these properties are shown in this article. Firstly, the corrosion behaviour of all coatings was evaluated through exposure tests in purified sodium for 5000 h at 400 °C. All coatings showed an acceptable corrosion behaviour in sodium. Finally, the friction and wear properties of one alloy candidate, NiCrBSi alloy, were studied in sodium in a dedicated designed facility. The influence of the oxygen concentration in sodium on the friction and wear properties was evaluated.

1 Introduction

Several zones in the Sodium-cooled Fast Reactors (SFRs) are in contact and undergo friction during reactor lifetime. The main examples are the insertion and removal of the assembly feet in their candles during fuel replacement or the movement of control rods into the reactor core during operation. During these operations, excellent friction coefficient and very low wear of the components are necessary. Beyond these properties, it is also necessary that the used materials have good compatibility in sodium, good mechanical behaviour, metallurgical stability, irradiation resistance, etc. Many studies have been carried out since the 1950s to determine the best possible pairs of material for all applications. The design of SFR prototypes has led to develop specific installations in order to measure the friction coefficient of pairs of materials and to evaluate wear during friction in sodium. The tribological behaviour of tens pairs of materials was evaluated and reported in literature as function of temperature [1], contact stress, roughness [1,2], sliding rate [1,3], irradiation [4], oxygen content in sodium [1,5] and other parameters. From this "material screening", feedbacks have shown that tribological hard coatings are most of the time necessary in order to limit the wear of the components and prevent them from jamming or blocking. Stellite 6®, a cobalt-base alloy containing hard phases, has been the most widely used coating in SFRs. Unfortunately, this alloy has the disadvantage of activating into high energy gamma emitter

* e-mail: fabien.rouillard@cea.fr

This is an Open Access article distributed under the terms of the Creative Commons Attribution License (http://creativecommons.org/licenses/by/4.0), which permits unrestricted use, distribution, and reproduction in any medium, provided the original work is properly cited.

Table 1. Weight chemical composition and main phases of the coatings, PTAW = Plasma Transferred Arc Welding and LC = Laser Cladding.

Hardfacing alloy	Process	Base	Cr	C	Si	B	Other	Main phases
CoCrW (eq. Stellite 6®)	PTAW	Co	28.3	1.1	1.1	0.0025	W: 4.7	Co-Cr solid solution dendrites + interdendritic [Co + Cr_7C_3] eutectic with primary tungsten and chromium carbides
	LC	Co	28.1	1.2	1.3	/	W: 4.8	Co-Cr solid solution dendrites + interdendritic [Co + Cr_7C_3] eutectic with primary tungsten and chromium carbides
NiCrBSi A	PTAW	Ni	12.7	0.4	3.4	2.1	/	Ni solid solution dendrites with binary eutectic [γ-Ni + Ni_3B] and chromium borides and carbides
	LC	Ni	12.6	0.3	3.5	2.2	/	Ni solid solution dendrites with binary eutectic [γ-Ni + Ni_3B] and chromium borides and carbides
NiCrBSi B	PTAW	Ni	12.7	0.4	3.3	1.8	/	Ni solid solution dendrites with binary eutectic [γ-Ni + Ni_3B] and chromium borides and carbides
NiMoCrSi	PTAW	Ni	15.5	0.04	3.4	/	Mo: 32.7	Ni solid solution + Laves Phase Mo-(Ni-Cr)-Si
	LC	Ni	16.4	0.04	3.7	/	Mo: 32.8	Ni solid solution + Laves Phase Mo-(Ni-Cr)-Si
NiCrSiWB	PTAW	Ni	9.6	0.7	5.0	0.5	W: 1.9	Ni solid solution dendrites with binary eutectic [γ-Ni + Ni_3Si] and nickel borides and chromium carbides
316L(N)	/	Fe	17.4	0.03	0.32	/	Ni: 12.2 Mo: 2.6	γ-Fe

^{60}Co hence leading to problems during maintenance and dismantling. As a consequence, research program on several hard nickel-base alloy coatings has been launched through a CEA-EDF-FRAMATOME collaboration. Firstly, their corrosion behaviour in purified sodium at 400 °C was studied up to 5000 h of exposure. This temperature corresponded to the operating temperature of the candles positioned at the bottom of the core. Then, in order to study their tribological behaviour in sodium, a low-scale sodium facility dedicated to tribological studies was developed at CEA-Saclay. The results obtained during the friction of 316L(N) − 316L(N) and 316L(N) − NiCrBSi alloy contacts in sodium at 200 °C were analyzed. Finally, the effect of oxygen concentration in sodium on the tribological behaviour was evaluated.

2 Materials and experimental procedure

2.1 Sodium preparation

The corrosion test was carried out into 2.4 L static sodium bath contained in molybdenum crucible. Molybdenum was used because it has a very low solubility in high-temperature sodium and corrodes very slowly [6]. The Mo crucible was placed in a nickel-base alloy reactor. In order to limit the pollution of sodium by oxygen, all sodium manipulations and the high-temperature corrosion test itself were carried out in a glove box flushed by high-purity argon. After sodium skimming, zirconium getter foil was inserted into the sodium bath then heated to 600 °C for several days in order to pump out any dissolved oxygen in sodium. With such procedure, the oxygen level in the sodium bath was decreased below 1 ppm in order to be as close as possible to the steady-state oxygen concentration evaluated in former French SFRs' primary sodium (<3 ppm) [7–9]. Once the sodium purification step was done, the nickel-base alloy reactor was opened and the coated specimens were put into the sodium bath with a new zirconium getter foil in order to ensure a very low oxygen concentration in sodium (<1 ppm) at any time of the corrosion test.

2.2 Samples and analytical techniques

2 mm-thick hardfacing alloys were coated on one single face of 316L(N) steel grade specimens (25 mm × 50 mm × 15 mm) in which our specimens (25 mm × 20 mm × 3 mm) were machined before exposition into purified liquid sodium at 400 °C for 500 h, 1000 h, 3000 h and 5000 h. The composition of the hardfacing alloy powders, the processes used for making the coatings and the main phases identified in the coatings are given in Table 1. All coatings were deposited

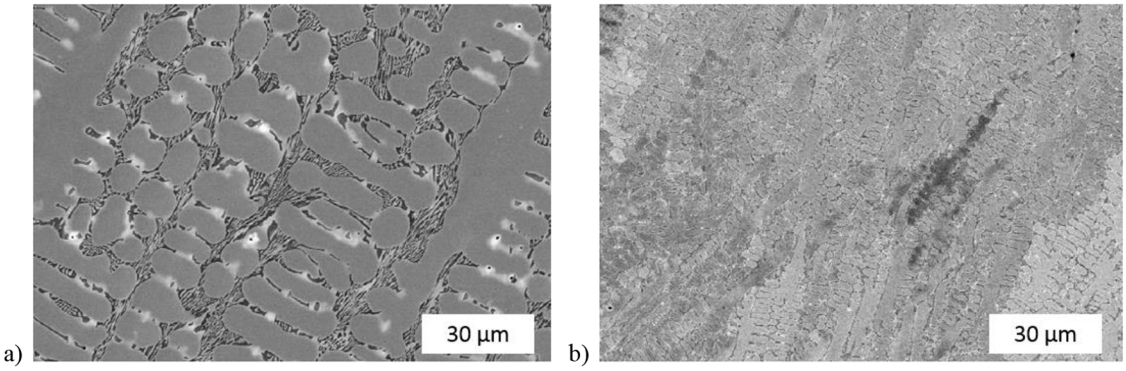

Fig. 1. FESEM images of CoCrW alloy cross-section deposited by (a) PTAW and (b) LC.

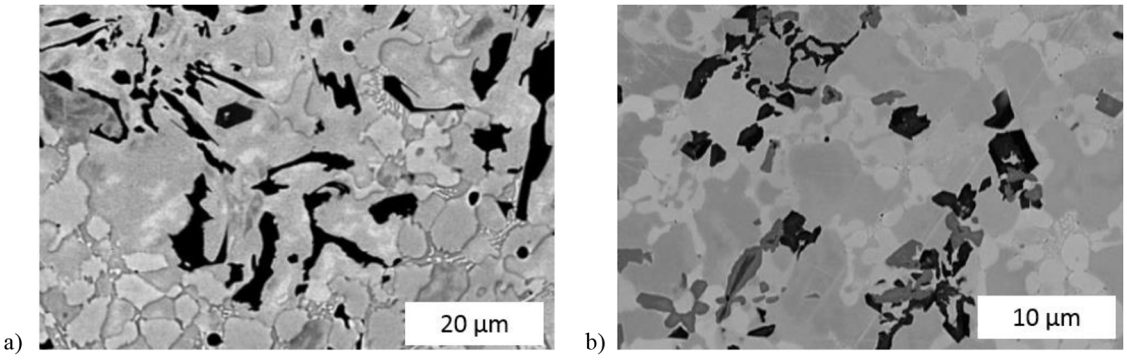

Fig. 2. FESEM images of NiCrBSi A alloy cross-section deposited by (a) PTAW and (b) LC.

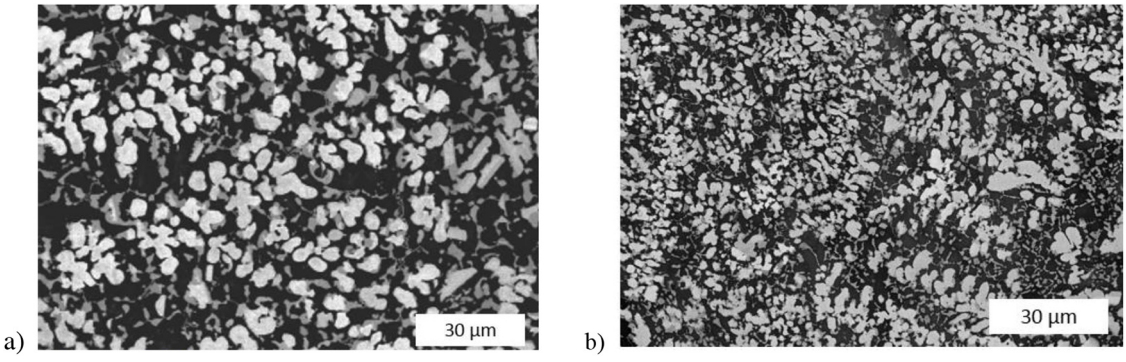

Fig. 3. FESEM image of NiMoCrSi alloy cross-section deposited by (a) PTAW and (b) LC.

by Plasma Transferred Arc Welding (PTAW) in industrial conditions. CoCrW, NiCrBSi A and NiMoCrSi were also deposited on 316L(N) substrate by Laser Cladding (LC) at CEA research lab. The different coating microstructures are strongly linked with the deposited energy used during processing. Coatings with a finer microstructure and a higher hardness could be obtained by the LC process thanks to its very high cooling rate. Hence, the size of the lamellar dendrites ($Co + Cr_7C_3$) formed in the CoCrW coating was about ten times lower when deposited by LC (Fig. 1). FESEM images of all the obtained coating cross sections are given in Figures 1–4. More details on the used coating processes and coating metallurgy are given in [10]. The surface of all coatings was grinded before corrosion and friction test. The arithmetic average roughness R_a of the coating surfaces was measured below $0.4\,\mu$m. After immersion, all the coupons were cleaned from sodium residues with the same well-controlled procedure: a first step in pure ethanol, then in water and then again in pure ethanol for 20 min in an ultrasonic bath. Sample weight

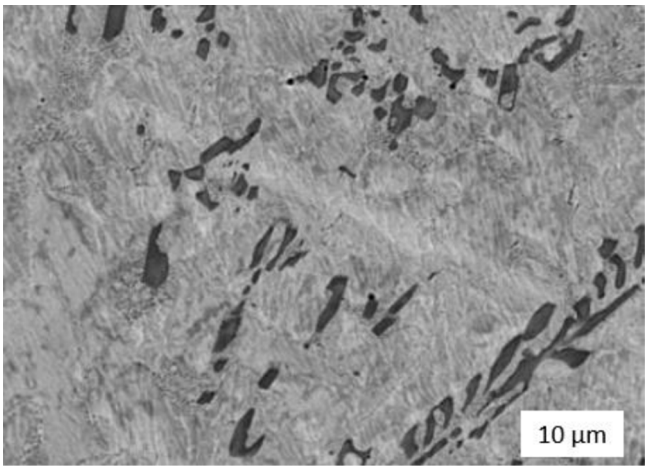

Fig. 4. FESEM image of NiCrSiW alloy cross-section deposited by PTAW.

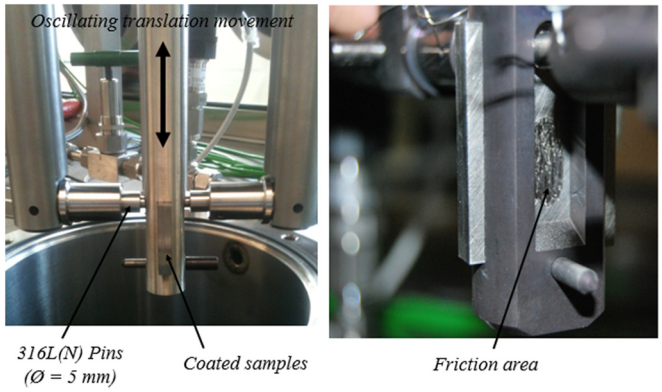

Fig. 5. Plate–plate uniaxial linear reciprocating-type tribometer.

Table 2. Friction tests.

Central specimens	Outer specimens	Environment	Operating temperature (°C)	Contact stress (MPa)	Rubbing speed (mm/s)	Total rubbing distance (m)
316L(N)	316L(N)	Argon	200	31	1	4
316L(N)	316L(N)	Purified sodium	200	31	1	4
NiCrBSi alloy B (PTAW)	316L(N)	Purified sodium	200	31	1	4
NiCrBSi alloy B (PTAW)	316L(N)	Non purified sodium	200	31	Variable	4

Purified sodium = [O] < 1 ppm; Non purified sodium = [O] > 10 ppm. The rubbing speed is defined as the speed at which the coated specimen moves relatively to the pin; the total rubbing distance is defined as the total distance travelled by the pin on the coated sample.

variation method was used for evaluating and ranking the corrosion resistance of all samples (mass difference error assessed to be 0.01 mg/cm^2). Finally, the samples were characterized by optical and Field Emission Scanning Electron Microscopy (FESEM). Modification of the surface composition at the sub-micron scale was carefully followed by Glow Discharge Optical Emission Spectroscopy (GDOES).

3 Tribological facility and tribological test procedure

In-sodium friction and wear tests were carried out using a plate–plate uniaxial reciprocating-type tribometer similar to the one presented in [3,11]. A photo of the facility is shown in Figure 5. The two outer pin specimens (5 mm in diameter) were made in 316L(N) steel grade for all friction tests and had flat shape. The central specimen was made of two back to back positioned coated or non-coated 316L(N) samples. The two outer 316L(N) pins were pressed against the central specimens by lever arms with the load applied by weights. During the friction test, the central specimen was moved up and down by the central pull rod. The friction force was recorded by a load cell and the dynamic friction coefficient μ were calculated by using equation: $\mu = \frac{F_T}{2 \times F_N}$ with F_T, the friction force and F_N, the normal force in Newtons. The normal applied force was accurately calibrated before test, thanks to in situ load-cells positioned in place of the outer specimens. The measurement uncertainty on the applied force given in Table 2 was estimated to be around 10%. Friction tests were carried out on 316L(N)–316L(N) and 316L(N)–NiCrBSi alloy B (PTAW) contacts. NiCrBSi alloy (whose trade name is Colmonoy 5®) has been identified by recent studies as a promising candidate to replace Stellite 6® [12,13]. The friction test parameters are detailed in Table 2. The chosen contact stress and rubbing speed values in the tests were of the same order of magnitude as the values calculated during operation in the reactor. In order to evaluate the influence of the oxygen concentration in sodium on the tribological behaviour of the tested materials, friction tests in purified and non-purified sodium were carried out. For the friction test in purified sodium, the specimens were heated in sodium containing zirconium strip at 600 °C for 3 days then cooled down at 200 °C before starting the friction test. This temperature, 200 °C, corresponds to the temperature at which the friction

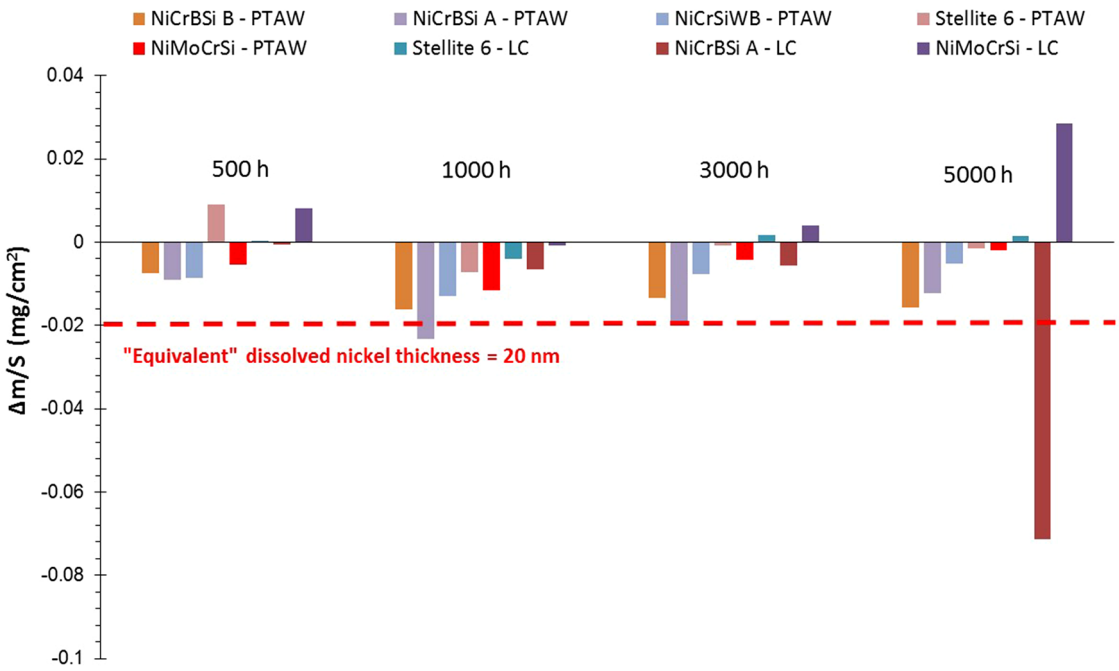

Fig. 6. Mass evolution (m(t)-m_0) of the coated samples after 5000 h at 400 °C in purified sodium – [O] < 1 ppm.

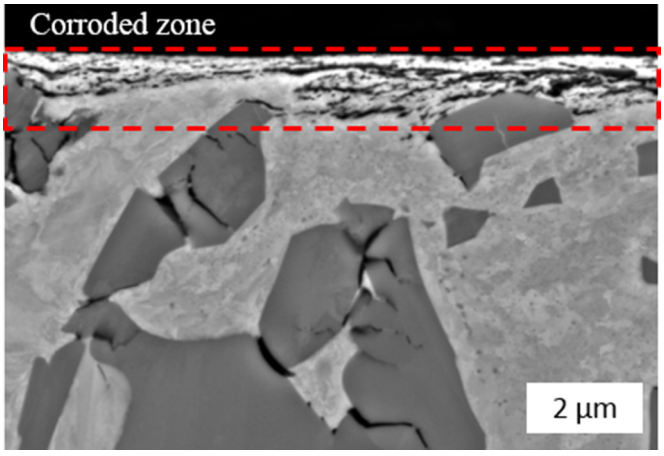

Fig. 7. FESEM image of NiCrBSi alloy A (PTAW) cross-section surface after exposure in sodium at 400 °C for 5000 h.

movement occurs between the assembly feet and the coated candles during fuel replacement. In this friction test, the oxygen concentration in sodium was estimated below 1 ppm [5,12,13]. For the friction test in non-purified sodium, the same procedure was carried out but without any zirconium strip in sodium. The oxygen concentration in the sodium bath in that case was measured between 10 and 20 ppm by sodium post-test purification procedure with zirconium getter foil.

4 Corrosion results and discussion

The time evolution of the coated sample weight after exposure at 400 °C in purified sodium is shown in Figure 6. All samples lost weight except NiMoCrSi and CoCrW alloys deposited by LC, which gained weight. It must be emphasized that the mass loss or mass gain for all coatings (except NiCrBSi A alloy deposited by LC) were extremely low: after 5000 h of exposure, the mass loss was lower than an equivalent 20 nm-thick dissolved nickel layer. Any dissolution kinetic determination was not possible given the uncertainties of measurements on weight evolution with time. The very low corrosion rate of the coatings was in good agreement with the low surface alteration observed macroscopically: the samples still appeared metallic coloured with the initial machining traces visible on their surface. The degraded zone at the surface of all coatings was observed by FESEM on cross sections. The larger degraded thickness layer was observed on the NiCrBSi alloy A (PTAW): a 1 μm thick porous zone formed at the surface after 5000 h (Fig. 7). This corrosion feature is in good agreement with the dissolution of the coating into the hot sodium bath.

The modification of the composition of the coatings at the surface was measured accurately with a high depth resolution by GDOES. For all coatings, the composition of these four elements appeared to vary on the surface: B, Cr, Si and Na. Figures 8–11 show the elementary composition evolution of the surface of NiCrBSi alloy B, CoCrW, NiCrSiW and NiMoCrSi surfaces deposited by PTAW on 316L(N) steel after exposure at 400 °C for 5000 h in sodium. The influence of the process of deposition on the corrosion behaviour is shown for NiCrBSi alloy A in Figures 12 and 13.

Firstly, boron was depleted on the surface of the boron-rich coatings NiCrBSi alloys A/B and NiCrSiWB alloy whatever the deposition process (PTAW or LC). The depth of boron depletion increased with exposure time.

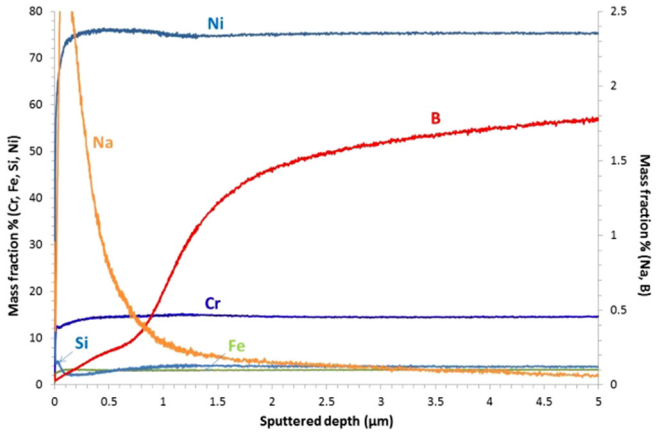

Fig. 8. Elementary profile of NiCrBSi alloy B (PTAW) surface after exposure in Na at 400 °C for 5000 h measured by GDOES.

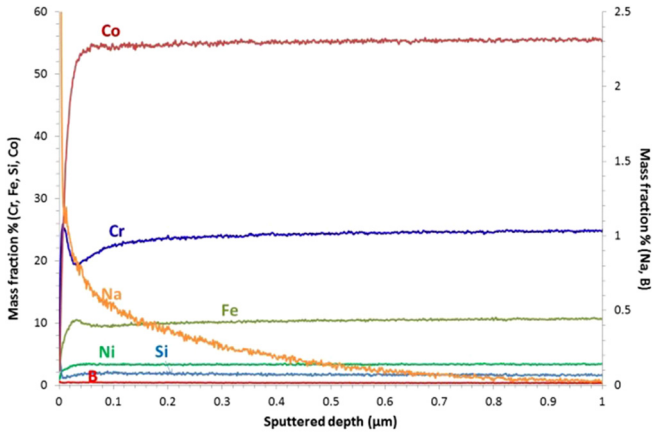

Fig. 9. Elementary profile of CoCrW alloy (PTAW) surface after exposure in Na at 400 °C for 5000 h measured by GDOES.

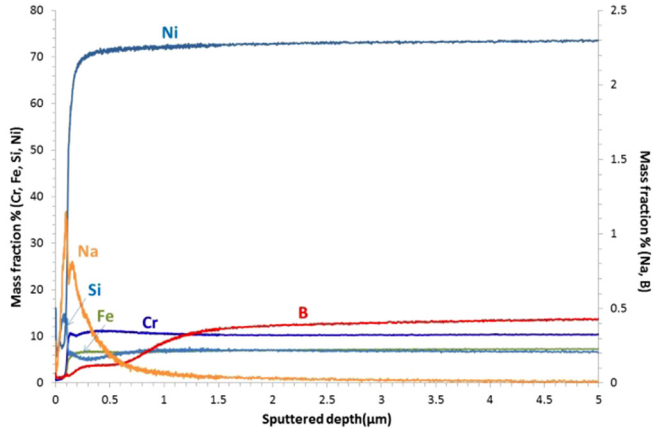

Fig. 10. Elementary profile of NiCrSiWB alloy (PTAW) surface after exposure in Na at 400 °C for 5000 h measured by GDOES.

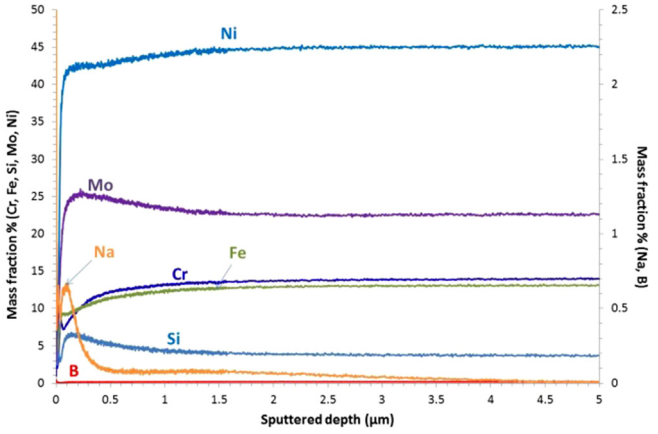

Fig. 11. Elementary profile of NiMoCrSi alloy (PTAW) surface after exposure in Na at 400 °C for 5000 h measured by GDOES.

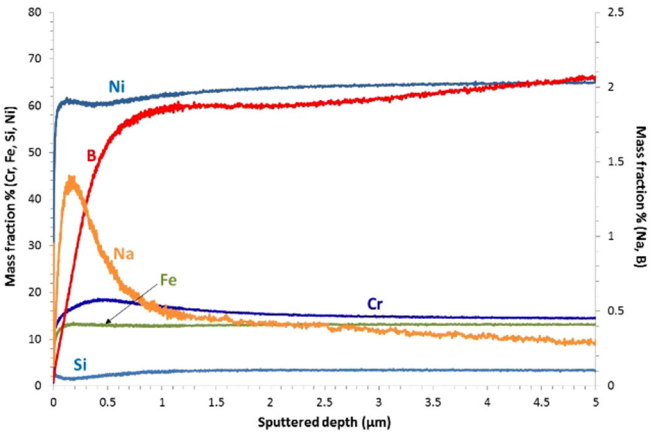

Fig. 12. Elementary profile of NiCrBSi alloy A (PTAW) surface after exposure in Na at 400 °C for 5000 h measured by GDOES.

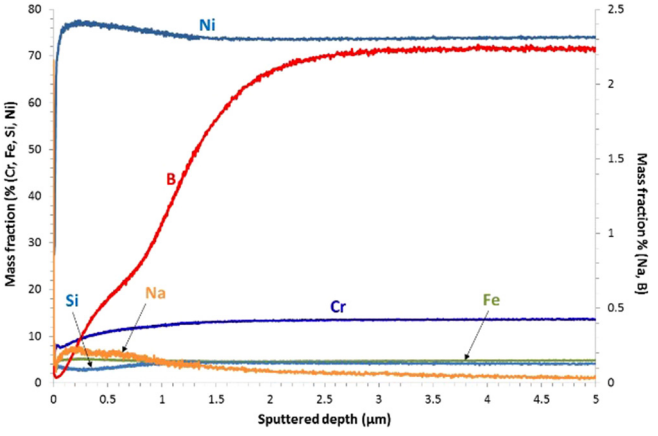

Fig. 13. Elementary profile of NiCrBSi alloy A (LC) surface after exposure in Na at 400 °C for 5000 h measured by GDOES.

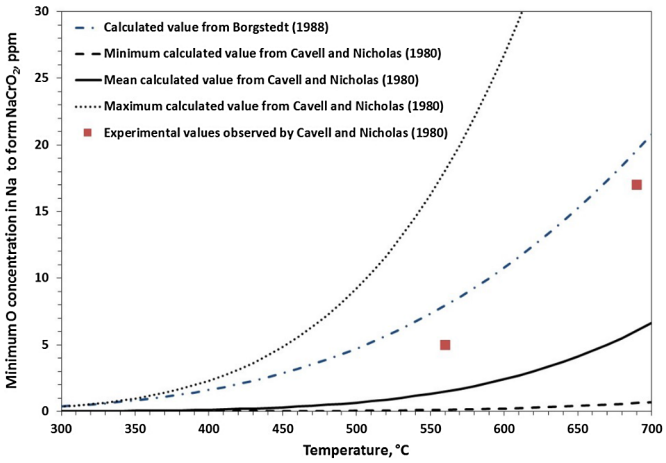

Fig. 14. Minimum oxygen concentration in sodium necessary to form $NaCrO_2$ on 316L stainless steel from literature data. For the calculated value from Borgstedt et al. [17], the activity of chromium in 316L(N) was taken from Azad et al. [18] and the enthalpy of formation of Na_2O and $NaCrO_2$ taken from Borgstedt et al. [17]. For all curves, the solubility law of oxygen in Na was taken from Noden et al. [19].

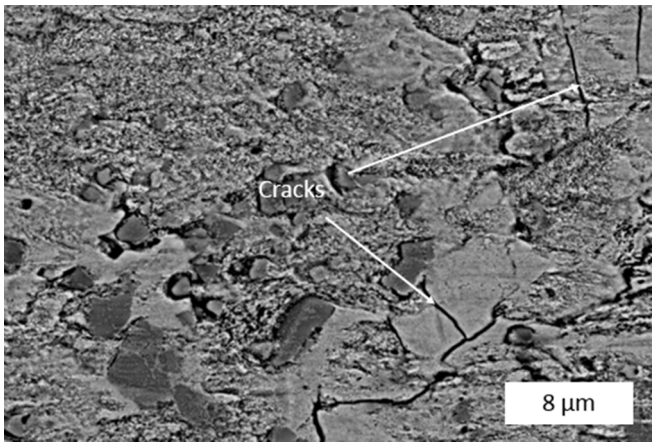

Fig. 15. Cracks formed on NiCrBSi alloy A (PTAW) surface before exposure in sodium observed by FESEM (surface).

Boron dissolution in sodium has already been observed for austenitic steels at 600 and 700 °C by Borgstedt et al. [14] even if the boron solubility law in sodium as a function of temperature is not well established in the literature [15]. The order of magnitude of the apparent diffusion coefficient of boron in the boron containing coatings, D_{app}, was calculated by fitting the measured boron depletion profiles with the solution of the 2nd Fick's law proposed for diffusion of species in a semi-infinite media and with a constant boron concentration at the coating surface equal to zero [16]. A D_{app} value around 10^{-15} cm^2/s was found. From this apparent diffusion coefficient, the maximum boron depleted zone thickness was evaluated to be around 30 μm after 60 yr at 400 °C which is quite reasonable.

Secondly, chromium was depleted in a thin zone (<0.5 μm) below the surface. For CoCrW alloy, this chromium depletion zone was clearly accompanied by a chromium-enriched zone at the sodium–coating interface (Fig. 9). This combined chromium enrichment and depletion on CoCrW alloy could indicate the formation of the ternary oxide $NaCrO_2$ on the coating surface. This ternary oxide is indeed known to be stable at low oxygen concentration in sodium. According to literature data, a minimum oxygen concentration value between 0.1 and 2 ppm is necessary to stabilize $NaCrO_2$ on 316L stainless steel (which contains about 17 wt.% of Cr) at 400 °C in Na (Fig. 14). This minimum oxygen concentration value to stabilize $NaCrO_2$ should be even lower for CoCrW alloy since this alloy contains a higher concentration of chromium, about 28 wt.%. Despite its likely presence, $NaCrO_2$ could not be detected on the surface of CoCrW alloy by XRD analysis, even using grazing angle, meaning that, if formed, its amount on the surface was very low and maybe discontinuous. The chromium enrichment observed on the surface of CoCrW alloy was hardly detectable for the other alloys in good agreement with the likely lower amount of $NaCrO_2$ formed on their surface because of the much lower chromium concentration contained in these alloys.

Finally, for the NiCrBSi and NiCrSiWB coatings, whatever the deposition process, the concentration of silicon was observed to slightly increase at the extreme surface and to be depleted underneath over a 0.5 μm-thick region. The origin of Si enrichment on the surface combined with its depletion underneath is unclear. It might reflect the formation of sodium silicate $NaSi_2O_5$ at the coating surface or the dissolution of Si in sodium followed by its re-deposition on the coating surface during the cooling of the sample [14]. The strong reactivity of silicon in hot sodium is quite known in literature. In particular, silicon and their oxides are soluble in sodium. The solubility of Si in sodium was estimated by interpolation around 100 molar ppm at 400 °C [14]. In consequence, its presence in the coating alloy should be detrimental for its corrosion behaviour. Nevertheless, it appeared that, at 400 °C, its influence on the degradation kinetics of the Si containing coatings was very low. The enrichment and depletion of silicon was not observed for NiMoCrSi alloy and CoCrW alloy in spite of the fact that they contained 3–4 wt.% and 1 wt.% of Si, respectively. This observation reveals that the reactivity of silicon depends on the microstructure and phase composition of the alloy. In particular, it could be proposed that Si dissolved in the nickel matrix, as it is the case for NiCrBSi and NiCrSiWB alloys, is more reactive (soluble) than Si contained in Laves phases as in NiMoCrSi alloy. Both boron and silicon dissolution in sodium participate to the mass loss of the coatings observed in Figure 6. For all coatings, the region where silicon and boron were depleted (depth <1 μm) contained a high concentration of sodium (>5 % mass) and micrometer-sized voids (Fig. 7). Sodium diffused even deeper in the NiCrBSi type coatings (about 15 μm). The penetration depth of sodium and its concentration were believed to be strongly linked to the density and depth of cracks and porosity formed on the coating surface during the process. This scenario is in good agreement with the highest density of cracks observed on the surface of the NiCrBSi type coating (Figs. 15 and 16). The sodium penetration depth was only around 2 μm for CoCrW alloy in good agreement with the absence of visible

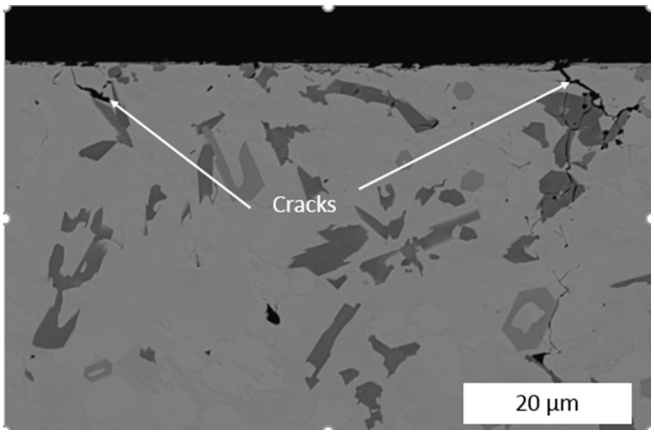

Fig. 16. Cracks formed on NiCrBSi alloy A (PTAW) surface before exposure in sodium observed by FESEM (cross section).

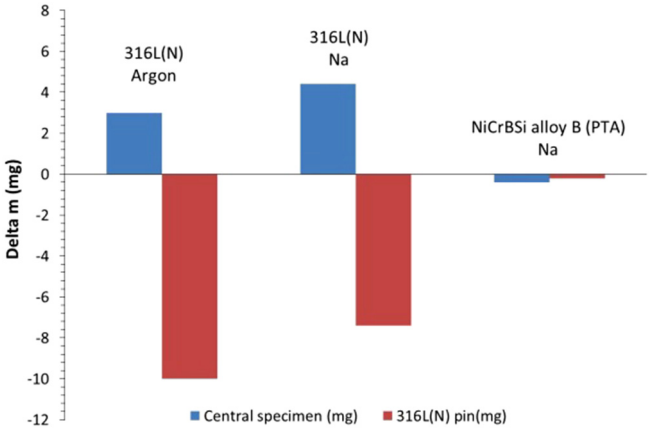

Fig. 17. Mass evolution of pin and central specimens for 316L (N)–316L(N) friction test in argon and sodium and for 316L(N)–NiCrBSi alloy B (PTAW) friction test in sodium at 200 °C under 31 MPa.

cracks on its surface. The higher weight gain observed for NiMoCrSi deposited by LC could also be explained as well by a higher penetration of sodium at the surface combined to a low dissolution rate. The influence of sodium penetration on the tribological properties in sodium is unknown and needs to be investigated. The deposition process had no impact on the corrosion kinetics of CoCrW alloy but affected that of NiCrBSi alloy A. The boron depletion was larger for NiCrBSi alloy A deposited by LC (Fig. 13) than deposited by PTAW (Fig. 12) in good agreement with its larger mass loss shown in Figure 6.

In conclusion, all tested hardfacing alloys showed relatively good compatibility in purified sodium at 400 °C up to 5000 h of exposure. This observation confirmed literature data indicating corrosion rates from 0.02 μm to 0.1 μm/yr for these alloy grades in flowing sodium at 400 °C [20]. If corrosion ranking has to be done, the best corrosion behaviour in sodium was observed for CoCrW alloy and NiMoCrSi alloys and the less corrosion resistant was for the NiCrBSi-type alloys in agreement, again, with literature

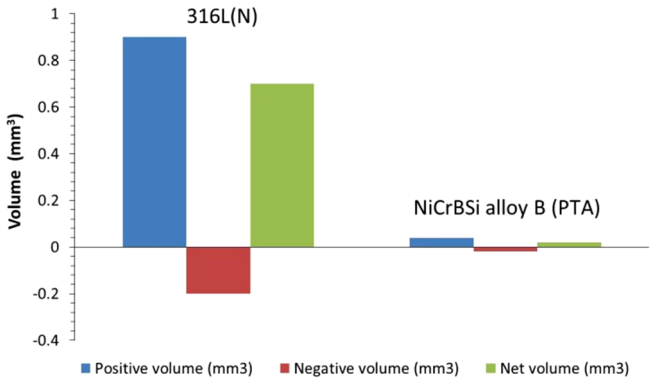

Fig. 18. Positive and negative volumes measured by 3D microscopy on the worn surface of the central specimen after friction test in sodium.

[21]. The lower corrosion resistance of NiCrBSi coatings is likely due to the presence of large amounts of boron and silicon in solid solution, two elements which are highly soluble in sodium.

5 Tribological behaviour in sodium

A comparison of the mass evolution of the specimens after friction tests of 316L(N) against itself and 316L(N) against NiCrBSi alloy B (PTAW) in purified sodium at 200 °C is shown in Figure 17. The wear resistance of both specimens (central specimen and outer pins) was higher when 316L (N) was rubbed against hardfacing NiCrBSi alloy. Very low mass transfer occurred during the 316L(N)–NiCrBSi friction test which contrasted with the 316L(N)–316L(N) friction test where steel was massively transferred from the outer pins to the central one (Fig. 17). This massive adhesive wear of 316L(N)–316L(N) contact was also observed when the friction test was carried out under inert gas indicating, thus, that this behaviour was not sodium dependent. The lower adhesive wear observed during the friction of 316L(N) on NiCrBSi alloy could be explained by the higher hardness of NiCrBSi alloy (585 ± 15 Hv1) than 316L(N) (200 ± 15 Hv1) (Fig. 18). In contrast, the friction coefficient measured during the 316L(N)–NiCrBSi alloy B friction test was higher than the one measured for the 316L(N)–316L(N) friction test (Fig. 19). No effect of the environment, purified Na or Argon, could be observed on the friction coefficient values measured for 316L(N)–316L(N) friction test (Fig. 19). This result was in good agreement with the fact that, in both environments, no lubricating oxide layer was formed on the steel surface.

As it can be observed in Figure 20, the oxygen concentration in sodium had an important effect on the tribological behaviour of the two specimens in contact and, more specifically, on the friction coefficient. The friction coefficient of 316L(N) against NiCrBSi alloy B (PTAW) was lowered by a factor of 1.5 by increasing the oxygen concentration in sodium from levels below 1 ppm (purified Na) to levels over 10 ppm (non-purified Na). This effect had already been observed in past studies and was mainly

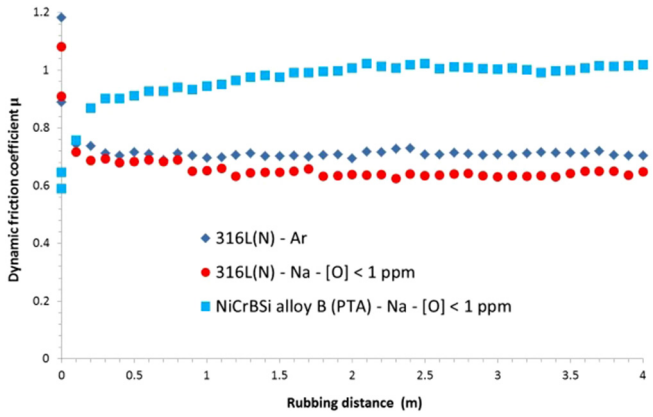

Fig. 19. Dynamic friction coefficient of 316L(N)–316L(N) and 316L(N)–NiCrBSi alloy B (PTAW) contact in purified sodium ([O] < 1 ppm) or argon at 200 °C under 31 MPa at 1 mm/s.

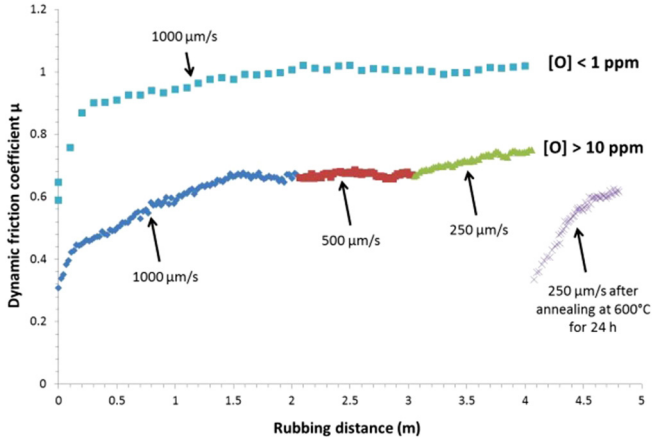

Fig. 20. Dynamic friction coefficient of 316L(N)–NiCrBSi alloy B (PTAW) contact in purified ([O] < 1 ppm) and non-purified sodium ([O] > 10 ppm) at 200 °C under 31 MPa.

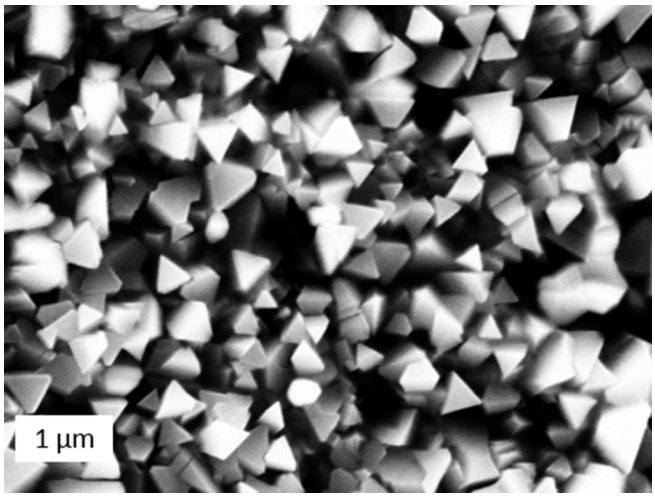

Fig. 21. FESEM image (secondary electron contrast) of the oxide crystals formed on the 316L(N) pin surface after annealing in oxygen-containing sodium at 600 °C for 24 h (Fig. 13).

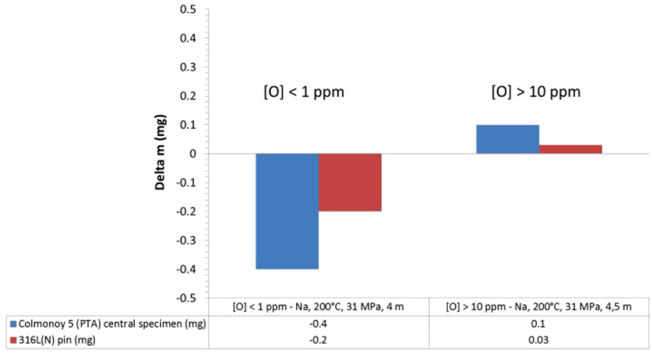

Fig. 22. Mass evolution of pin (red) and central specimens (blue) for 316L(N)–NiCrBSi alloy B (PTAW) friction test in purified and non-purified sodium at 200 °C under 31 MPa.

attributed to the formation of lubricating oxide such as chromite ($NaCrO_2$) on the surface of the steels [2,5,22]. This proposed beneficial effect of surface oxide layer on the samples was evaluated by carrying out a complementary friction test at 200 °C after annealing the specimens in non-purified sodium ([O] > 10 ppm) at 600 °C for 24 h. The friction coefficient decreased drastically to a value close to 0.3 then increased progressively with rubbing distance to its initial value, around 0.7. This time evolution of the friction coefficient was in good agreement with the formation of a lubricating oxide layer after exposure at high temperature in non-purified sodium and its progressive removal by friction ending up with metal–metal contact friction. This assumption was confirmed by the observation of chromium-rich oxide on the surface of the 316L(N) pin after annealing test (Fig. 21). The exact nature of the formed oxide crystals was not identified by XRD but it was proposed that these oxide crystals were $NaCrO_2$ owing to the fact that they were rich in chromium and their morphology was very similar to the $NaCrO_2$ crystals identified by Cavell et al. after exposing AISI 316 stainless steel in static sodium containing 1–24 wppm of oxygen at 450–675 °C [23].

The formation of chromite at 600 °C in sodium containing more than 10 wpm of oxygen was in good agreement with the minimum oxygen concentration proposed in literature for its formation, about 10 wpm at 600 °C (Fig. 14). Two scenarios have been proposed in literature to explain the beneficial effects of chromite on the friction coefficient. On one hand, Nicholas and Cavell [22] have proposed that the mechanism involved in chromite lubrication is the deposition on the surface of oriented crystals which shear and form a low shear-strength oriented layer somewhat like that usually proposed in graphite lubrication. On the other hand, Radcliffe considered this last mechanism unnecessarily complex and has proposed that chromite simply acts by reducing adhesion and junction growth during rubbing [5].

Finally, it was observed that the wear resistance of the rubbing contact was also slightly improved with the oxygen concentration in sodium (Fig. 22). More friction tests are needed to confirm this tendency.

6 Conclusions

Several nickel-base alloys were evaluated as candidates for hardfacing alloys in SFRs. All of them showed good chemical compatibility in sodium at 400 °C for at least 5000 h, whatever the deposition process (Plasma Transferred Arc Welding or Laser Cladding). In-sodium friction tests revealed better wear behaviour for 316L(N)–NiCrBSi alloy contact than for 316L(N)–316L(N) contact. However, the measured friction coefficient was slightly higher. The beneficial influence of increasing the oxygen concentration in sodium on the friction coefficient, already demonstrated in literature, has been confirmed. Friction tests with all the hardfacing nickel base alloy candidates are needed at various stress contacts, sliding velocities and temperature for identifying the best alternative to Stellite 6® in SFRs.

This project was supported and funded by CEA, FRAMATOME and EDF within the ASTRID project.

Author contribution statement

F. Rouillard has written the article and has leaded the experimental campaign. B. Duprey has carried out the experiments in sodium. M. Tabarant has made the GDOES analyses. P. Aubry and C. Blanc have provided the coatings deposited by laser and made their metallurgical characterization. The other co-authors have contributed to this work by providing support, proofreading and expert viewpoints on the different topics discussed in the article.

References

1. E. Wild, K.J. Mack, M. Gegenheimer, *Liquid Metal Tribology in Fast Breeder Reactors* (Kernforschungszentrum, Karlsruhe, 1984)
2. R.N. Johnson, R.C. Aungst, N.J. Hoffman, M.G. Cowgill, G.G. Whitlow, W.L. Wilson, Development of low friction materials for LMFBR components, in M.H. Cooper (Ed.), *Proceeding in First International Conference on Liquid Metal Technology in Energy Production*, 1976, Champion, p. 122
3. E. Wild, K.J. Mack, Friction and wear in liquid-metal systems: compatibility problems of test results obtained from different test facilities, in M.H. Cooper (Ed.), *Proceeding in First International Conference on Liquid Metal Technology in Energy Production*, 1976, Champion, p. 131
4. G.A. Whitlow, W.L. Wilson, T.A. Galioto, R.L. Miller, S.L. Schrock, N.J. Hoffman, J.J. Droher. R.N. Johnson, Corrosion and tribological investigations of chromium carbide coatings for sodium cooled reactor applications, in M.H. Cooper (Ed.), *Proceeding in First International Conference on Liquid Metal Technology in Energy Production*, 1976, Champion, p. 138
5. S.J. Radcliffe, Friction coefficient of AISI 316 stainless steel in impure and in zirconium hot-trapped sodium, in: D. Dowson (Ed.), *Proceeding of the 7th Leeds-Lyon Symposium on Tribology, Institute of Tribology*, p. 64
6. H. Borgstedt, C.K. Mathews, *Applied Chemistry of the Alkali Metals* (Kluwer Academic/Plenum Publishers, Dordrecht, 1987)
7. J. Guidez, B. Bonin, *Réacteurs nucléaires à caloporteur sodium* (2014)
8. J-L. Courouau, F. Balbaud-Célérier, V. Lorentz, T. Dufrenoy, Corrosion by liquid sodium of materials for sodium fast reactors: the CORRONa testing device, in *Proceeding in International Congress on Advances in Nuclear Power Plants (ICAPP '11)*, Nice, France, 2011, p. 2
9. J. Guidez, *Phénix: The experience feedback* (EDP Sciences, Paris, 2013)
10. G. Rolland, C. Cossange, A. Andrieu, M. Blat-Yrieix, P. Sallamand, M. Duband, C. Blanc, P. Aubry, F. Rouillard, T. Marlaud, Coating toughness estimation through a Laser Shock Testing in Ni-Cr-B-Si-C Coatings, Mater. Sci. Forum **941**, 1886 (2018)
11. H. Kumar, V. Ramakrishnan, S.K. Albert, C. Meikandamurthy, B.V.R. Tata, A.K. Bhaduri, High Temperature wear and friction behaviour of 15Cr-15Ni-2Mo titanium-modified austenitic stainless steel in liquid sodium, Wear **270**, 1 (2010)
12. A.K. Badhuri, R. Indira, S.K. Albert, B.P.S. Rao, S.C. Jain, S. Asokkumar, Selection of hardfacing material for component of the Indian Prototype Fast Breeder Reactor, J. Nucl. Mater. **334**, 109 (2004)
13. H.U. Borgstedt, G. Frees, G. Drechsler, Korrosions reaktionen sauerstoffempfindlicher Metalle in flüssigem Natrium mit Oxidgehalten. I. Reaktionen von Zirkonium und Zircaloy2, Werstoffe und Korrosion **21**, 568 (1970)
14. H.U. Borgstedt, G. Frees, H. Schneider, Corrosion and creep of pressurized stainless-steel tubes in liquid-sodium at 873 and 973 K, Nucl. Technol. **34**, 290 (1977)
15. H.U. Borgstedt, C. Guminski, IUPAC-NIST Solubility Data Series. 75. Nonmetals in Liquid Alkali Metals, J. Phys. Chem. Ref. Data **30**, 835 (2001)
16. J. Crank, *The Mathematics of Diffusion*, 2nd edn. (Oxford Science Publications, Oxford, 1975)
17. N.P. Bhat, H.U. Borgstedt, Corrosion behaviour of structural materials in sodium influenced by formation of ternary oxides, Werkstoffe und Korrosion **39**, 115 (1988)
18. A.M. Azad, O.M. Sreedharan, J.B. Gnanamoorthy, A novel determination of thermodynamic activities of metals in an AISI 316 stainless steel by a metastable emf method, J. Nucl. Mater. **144**, 94 (1987)
19. J.D. Noden, A general equation for the solubility of oxygen in liquid sodium, J. Br. Nucl. Energy Soc. **12**, 57 (1973) [Addendum J. Br. Nucl. Energy Soc. **12**, 329 (1973)]
20. E. Yoshida, Y. Hirakawa, S. Kano, I. Nihei, In-sodium tribological study of cobalt-free hard facing materials for contact and sliding parts of FBR components, in *SFEN,*

Proceeding in the Fourth International Conference on Liquid Metal Engineering and Technology, Avignon, 1998, paper 502

21. S. Kano et al., Investigation of tribological phenomena in sodium for LMFBR, in J.M. Dahlke (Ed.), *Proceeding in the Second International Conference on Liquid Metal and Technology in Energy Production*, Richland 1980, paper 3–60
22. M.G. Nicholas, I.W. Cavell, The formation of chromite on AISI 316 and other chromium containing alloys, in J.M. Dahlke (Ed.), *Proceeding in the Second International Conference on Liquid Metal Technology in Energy Production*, Richland, 1980, paper 3–35
23. I.W. Cavell, M.G. Nicholas, Some observations concerned with the formation of chromite on AISI 316 exposed to oxygenated sodium, J. Nucl. Mater. **95**, 129 (1980)

Cite this article as: Fabien Rouillard, Brigitte Duprey, Jean-Louis Courouau, Raphaël Robin, Pascal Aubry, Cécile Blanc, Michel Tabarant, Hicham Maskrot, Laetitia Nicolas, Martine Blat-Yrieix, Gilles Rolland, Thorsten Marlaud, Evaluation of cobalt free coatings as hardfacing material candidates in sodium-cooled fast reactor and effect of oxygen in sodium on the tribological behaviour, EPJ Nuclear Sci. Technol. **5**, 10 (2019)